applied sciences

MDPI

Article

Terrain Surface Interpolation from Large-Scale 3D Point Cloud Data with Semantic Segmentation in Earthwork Sites

Suyeul Park [1], Yonggun Kim [2] and Seok Kim [1,*]

[1] Department of Railroad Infrastructure Engineering, Korea National University of Transportation, Seoul 16106, Kyeonggi-do, Republic of Korea; sypark@ut.ac.kr
[2] Department of Railroad Convergence System, Korea National University of Transportation, Seoul 16106, Kyeonggi-do, Republic of Korea; xpdlvm090100@ut.ac.kr
* Correspondence: kimseok@ut.ac.kr

Abstract

Over the past few years, various research has been conducted to utilize 3D point cloud data in construction sites. This is because 3D point cloud data contain a variety of information, such as spatial coordinates (X, Y, Z), intensity, and color (RGB), making them highly applicable to construction environments that require precise operations. Accordingly, this research developed a new terrain surface interpolation method that leverages diverse information embedded in large-scale 3D point cloud data acquired from earthwork sites, as part of a foundational study for construction automation. In particular, the proposed terrain surface interpolation method was designed to be integrated with semantic segmentation based on 3D point cloud data, with a focus on enhancing the accuracy of earthwork volume estimation. Furthermore, field experiments were conducted using heavy construction equipment to compare terrain change and earthwork volume analyses between 3D point cloud data with and without the application of the proposed interpolation method. The analysis results of earthwork volumes indicated that the application of the terrain interpolation method to 3D point cloud data for construction equipment reduced estimation errors by approximately 94% compared to non-interpolated data. These findings demonstrate the effectiveness of the proposed method and are expected to contribute to future research in artificial intelligence and robotics utilizing 3D point cloud data within the construction industry.

Keywords: 3D point cloud data; terrain surface interpolation; earthwork volume estimation; heavy construction equipment; change detection analysis; semantic segmentation

check for updates

Academic Editor: Asterios Bakolas

Received: 14 October 2025
Revised: 23 November 2025
Accepted: 25 November 2025
Published: 4 December 2025

Citation: Park, S.; Kim, Y.; Kim, S. Terrain Surface Interpolation from Large-Scale 3D Point Cloud Data with Semantic Segmentation in Earthwork Sites. *Appl. Sci.* **2025**, *15*, 12831. https://doi.org/10.3390/app152312831

Copyright: © 2025 by the authors. Licensee MDPI, Basel, Switzerland. This article is an open access article distributed under the terms and conditions of the Creative Commons Attribution (CC BY) license (https://creativecommons.org/licenses/by/4.0/).

1. Introduction

Accurate estimation of earthwork volume is a critical component of construction project management, particularly in terms of cost control and schedule management. In road construction projects, where earthwork such as embankment and excavation occupies a significant proportion of the total work, the accuracy of earthwork volume estimation becomes even more influential. Consequently, extensive research has been conducted in the construction industry on accurate earthwork volume estimation, which has significantly contributed to the advancement of surveying instruments and measurement technologies [1–3].

Traditionally, electronic surveying instruments such as total stations were primarily used for earthwork measurement in construction projects. However, in recent years, the

utilization of advanced digital technologies such as Unmanned Aerial Vehicles (UAVs) and the Global Navigation Satellite System (GNSS) has been increasing [4–7]. The photogrammetric method using UAVs offers the advantage of easily acquiring data over wide areas, which makes it particularly useful for large-scale projects such as road construction [4,8]. Nevertheless, UAV-based photogrammetry tends to exhibit lower vertical accuracy (i.e., the accuracy of the absolute Z-coordinate) compared to ground-based LiDAR, especially when GNSS or Ground Control Points (GCPs) are not employed. Therefore, numerous research have been conducted to compensate for this limitation [9].

Beyond image-based photogrammetry, other research efforts have focused on transforming 2D image data into 3D representations. These methods utilize GNSS-based absolute coordinates to generate 3D point cloud data, which is now widely adopted in the construction industry. Since 3D point cloud data include precise spatial information in the X, Y, and Z axes, they are more suitable for construction environments that demand high accuracy [10–21].

However, despite the advantages of 3D point cloud data in providing accurate spatial information, processing large-scale datasets from construction sites—such as noise and outlier removal, registration, and 3D labeling—requires significant time and computational effort. Moreover, accurate earthwork volume estimation from such massive 3D point cloud data remains a challenging task. This is because, during UAV-based data acquisition, not only the terrain but also construction workers, heavy construction equipment, and various materials are simultaneously captured, all of which can negatively affect the accuracy of volume estimation. These heterogeneous objects are major factors that interfere with the precise estimation of earthwork quantities [4].

To address these challenges, this research proposes a new earthwork volume estimation approach that integrates 3D point cloud data–based semantic segmentation and terrain surface interpolation methods. The proposed method aims to overcome the limitations of conventional approaches, in which unnecessary objects are included in the estimation process. Specifically, this study introduces an interpolation-based method that efficiently reconstructs the ground surface by leveraging both the semantic information derived from 3D semantic segmentation and the spatial characteristics of 3D point cloud data corresponding to heavy construction equipment.

This research focuses on the development and application of a terrain surface interpolation method using large-scale 3D point cloud data acquired from an earthwork construction site. The experiment testbed was a road construction project located in the Republic of Korea, which was in the earthwork phase at the time of UAV data acquisition. For the efficient progress of this research, the 3D heavy construction equipment dataset and 3D semantic segmentation model, developed in previous studies [22,23], were utilized, while the terrain surface interpolation method was newly developed in this research. In addition, the 3D point cloud data from the road construction site, which were used as the test dataset for the semantic segmentation model, were also generated in this research. The test dataset for the 3D semantic segmentation model consisted of large-scale 3D point cloud data captured using UAV and was labeled into three classes: Class 1 (Ground), Class 2 (Non-ground), and Class 3 (Heavy Construction Equipment, HCE). The data used for terrain interpolation and 3D semantic segmentation in this research consist of large-scale 3D point clouds in the Semantic3D dataset [24,25]. In this research, the data utilized for performing terrain interpolation and 3D semantic segmentation had dimensions equal to or smaller than 600 m $\times$ 510 m $\times$ 90 m in width, length, and height, respectively, with each file being $\leq$500 MB and containing $\leq$50,000,000 points. The proposed terrain surface interpolation method was applied using the same test dataset employed for the semantic segmentation model. Finally, for the analysis of terrain change and earthwork volume

estimation, this study utilized the 3D point cloud data processed with the developed terrain surface interpolation method. In this research, only the object-recognized data belonging to Class 1 and Class 3 were used for terrain interpolation, whereas Class 2 was excluded from the scope of this research.

In terms of methodology, the overall workflow of this research was as follows. First, UAV-based photogrammetry was performed to capture the road construction site in the earthwork phase, and the acquired imagery was processed to generate 3D point cloud data. These data were preprocessed through denoising and filtering procedures and then used as test data for the previously developed 3D semantic segmentation model. Among the predicted outputs of the model, the 3D point cloud data corresponding to Class 3 (HCE) were used for the terrain surface interpolation process. Unlike conventional interpolation methods [26] that remove and regenerate 3D data, the proposed method adjusts the height values of the heavy construction equipment point clouds predicted by the 3D semantic segmentation model so that their elevation aligns with that of the surrounding ground surface. After completing the terrain surface interpolation, time-series 3D point cloud data were analyzed to evaluate terrain changes. Subsequently, comparative analyses were performed between interpolated datasets to assess both change detection and earthwork volume estimation. This research is particularly significant in that it proposes an efficient terrain surface interpolation method that leverages the 3D semantic segmentation results from large-scale 3D point cloud data acquired at actual earthwork sites. This new interpolation method adjusts the elevation values of 3D point clouds representing heavy construction equipment rather than deleting them, thereby improving computational efficiency and maintaining spatial continuity in terrain reconstruction.

2. Related Works

2.1. Earthwork Volume Estimation Method

To estimate earthwork volume at construction sites using orthophotographs acquired by UAVs, the imagery is generally converted into 3D point cloud data and subsequently processed to construct a Digital Elevation Model (DEM) [20]. In this process, the point cloud data are organized into triangular surfaces based on a Triangulated Irregular Network (TIN), where the Delaunay triangulation algorithm is applied to maintain topological adjacency without intersection among neighboring points [27,28]. The generated irregular triangular mesh is then superimposed onto an X–Y grid, forming rectangular prisms within each cell. Subsequently, the Z-values are assigned to each square cell to determine the height of the rectangular prism, and the final earthwork volume is calculated by summing the volumes obtained through this iterative process [29]. In addition to the TIN-based method, the Grid-based method is also widely used for earthwork volume estimation. The Grid-based method is known to be more efficient for large-scale 3D point cloud data because it offers shorter processing times and higher numerical stability compared to the TIN-based approach [28]. For this reason, major 3D point cloud processing software such as Leica Cyclone 3DR [30], Trimble RealWorks [31], and CloudCompare [32] have adopted the 2.5D Volume algorithm, a type of grid-based method, for the computation of earthwork quantities in large datasets.

The 3D TIN-based method, one of the most commonly used methods for 3D point cloud–based earthwork volume estimation, can accurately reflect local terrain characteristics; however, it becomes computationally expensive and inefficient when processing large datasets. In contrast, the 2.5D Volume algorithm assumes a single Z-value for each X–Y coordinate pair in a raster-based framework, providing high computational efficiency and shorter processing times when applied to large-scale datasets [28]. Previous studies on UAV-based DEMs have also demonstrated that the 2.5D Volume algorithm achieves

accuracy comparable to GNSS-RTK survey results while maintaining high computational efficiency [29]. Therefore, considering the extensive area characteristics of earthwork sites, this research adopts the 2.5D Volume algorithm as an appropriate and efficient method for estimating earthwork volume over wide construction areas.

2.2. Terrain Surface Interpolation Method

In general, for the terrain interpolation of 3D point cloud data, the Delaunay triangulation algorithm based on a Triangulated Irregular Network (TIN) is widely utilized [8]. This method constructs a triangular mesh by connecting the nearest neighboring points in the point cloud and is commonly applied in UAV-based earthwork volume estimation studies as well as in commercial 3D data processing software. However, the Delaunay triangulation approach may produce uneven or distorted surfaces, and in certain cases, irregular triangles may be generated. In particular, in areas where the point cloud data are missing (holes), only mesh surfaces are formed, without the generation of actual 3D point data, thereby limiting its applicability [4,26,33].

To overcome these limitations identified in previous studies, Nguyen et al. (2016) [26] proposed a method that performs terrain interpolation without converting point clouds into mesh structures, instead directly interpolating the missing regions within the point cloud space. This approach generates new 3D point cloud data to fill the holes for terrain surface interpolation. Unlike mesh-based hole-filling methods, this method identifies the boundary of the hole and generates new 3D point clouds by applying tangent values corresponding to the elevation of the boundary points. Moreover, by applying elevation values to the hole boundaries, the algorithm enables adaptive interpolation in highly variable terrain conditions. Compared with the Delaunay triangulation approach, The height-based interpolation method can effectively generate 3D point cloud data across complex terrain surfaces with multiple planes, thereby improving the continuity of the interpolated surfaces.

Accordingly, by analyzing the findings of the literature review, this research identified the key considerations necessary for developing a new terrain surface interpolation method. These considerations address the specific characteristics of earthwork construction sites represented by large-scale 3D point cloud data, including the need to generate points uniformly within missing regions and to minimize data loss during the interpolation process. In addition, state-of-the-art 3D point cloud-based semantic segmentation algorithms with superior object recognition performance are applied to further enhance the performance of the proposed terrain interpolation method [24,34–37]. Based on these considerations, a novel method capable of performing terrain surface interpolation on large-scale 3D point cloud datasets obtained from earthwork sites is developed.

3. Development of Terrain Surface Interpolation Method and Selection of Earthwork Volume Estimation Approach

3.1. Overview

The terrain surface interpolation method developed in this research utilizes both the predicted data obtained from semantic segmentation of heavy construction equipment based on 3D point cloud data and the inherent characteristics of the 3D point cloud data itself. Unlike the conventional method [26] that deletes and regenerates 3D point cloud data, the proposed interpolation method leverages the predicted semantic segmentation data to adjust the elevation values of the 3D point cloud data, thereby introducing a distinct and innovative approach compared to previous studies. As shown in Figure 1, the overall procedure of the proposed terrain surface interpolation method is as follows. First, a semantic segmentation training model for heavy construction equipment is constructed

using 3D point cloud data, and the corresponding prediction results are generated. Next, the predicted data obtained from the semantic segmentation model is applied to perform terrain interpolation on the 3D point cloud data. Finally, the 3D point cloud data interpolated through this process is used to calculate and verify the earthwork volume using 3D processing software (CloudCompare v2.12 alpha).

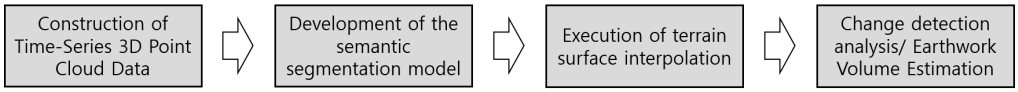


Figure 1. Process of the terrain surface interpolation method.

3.2. Semantic Segmentation of Large-Scale 3D Point Cloud Data from Earthwork Sites

In this research, the terrain surface interpolation process utilizes the predicted data generated from the semantic segmentation model trained on large-scale 3D point cloud data of earthwork sites. The purpose of applying this approach is to minimize errors caused by large, unnecessary objects such as heavy construction equipment and construction materials that are often included during earthwork volume estimation. In particular, by applying 3D semantic segmentation, objects located on the 3D point cloud data of earthwork sites can be automatically classified. This automated classification enables the terrain surface interpolation to be performed more efficiently than traditional manual interpolation methods.

For this purpose, this study utilized the previous research [23] on the development of a semantic segmentation model based on large-scale 3D point cloud data from earthwork sites, while the terrain surface interpolation method itself was developed in this study to enhance overall research efficiency. The semantic segmentation model applied in this research was trained using the SCF-Net algorithm, which showed the best performance in recognizing heavy construction equipment among the tested models, achieving an IoU_{c3} (Intersection-over-Union for Class 3) value of 89.5% [23,34]. The labeling applied in this study consisted of three classes defined in the 3D point cloud–based semantic segmentation dataset: Class 1—Ground, Class 2—Non-ground, and Class 3—HCE.

To prepare the data for terrain surface interpolation, the trained 3D point cloud–based semantic segmentation model was applied to the newly constructed 3D point cloud data (test data) of the earthwork site, and corresponding predicted label data were generated. The test data used for training the semantic segmentation model contained multiple data fields (X, Y, Z, I, R, G, and B), allowing one-to-one matching between the predicted label data (*.LABELS) and each point in the raw point cloud. Consequently, this study combined the input data (*.TXT) and the corresponding prediction results (*.LABELS) into a single dataset to construct large-scale 3D predicted point cloud data (*.TXT) incorporating semantic segmentation results.

3.3. Development of Terrain Surface Interpolation Method

Next, this research performed terrain surface interpolation using the predicted data generated from the semantic segmentation of heavy construction equipment. Unlike conventional approaches [26] that delete and regenerate object 3D point cloud data, the method developed in this research adjusts the elevation of objects by utilizing the prediction information obtained from the semantic segmentation results. Since all points in the predicted data generated by the 3D semantic segmentation model possess class values ranging from Class 1 to Class 3, the proposed terrain surface interpolation method was designed to take advantage of these class characteristics when performing surface reconstruction.

The key concept of the proposed interpolation method is illustrated in Figure 2. As shown in Figure 2a, the 3D predicted data generated by the semantic segmentation model

includes both ground points (Class 1, blue) and heavy construction equipment points (Class 3, red). Each point in the experimental 3D predicted dataset contains the data fields X, Y, Z, I, R, G, B, and C, and the proposed terrain surface interpolation method utilizes this class information. Specifically, as illustrated in Figure 2a, the proposed method interpolates the terrain by adjusting the Z-values of heavy construction equipment points based on their class information within mixed-class 3D point cloud data. Unlike conventional approaches that remove heavy construction equipment point clouds, the proposed terrain surface interpolation method retains these points and uses their class-based attributes. As shown in Figure 2b, the Z-values of heavy construction equipment points (red) located within a specified cluster radius (r) are adjusted to match the elevation of surrounding ground points (blue). Through this process, the proposed method achieves terrain interpolation without deleting object data, thereby preserving spatial continuity and improving computational efficiency.

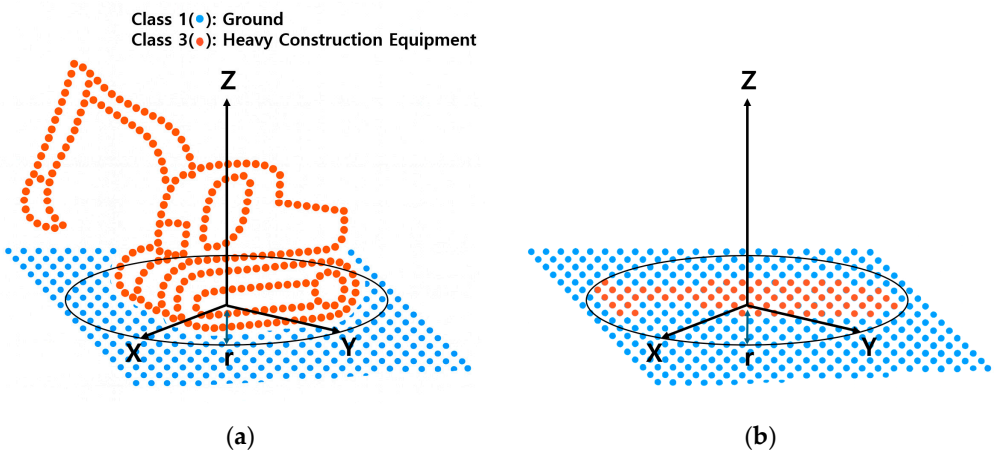


Figure 2. Concept of the Terrain Surface Interpolation Method. (**a**) Before Terrain Surface Interpolation. (**b**) After Terrain Surface Interpolation.

Specifically, the distinction of the terrain surface interpolation approach developed in this research lies in its adjustment of the elevation of all objects present in the 3D point cloud data processed with semantic segmentation, rather than deleting and regenerating object data. As shown in Figure 2a, the proposed method first calculates the centroid of each heavy construction equipment (classified as Class 3) by averaging the X and Y coordinates of the identified points. A circular cluster with a defined radius (r) is then generated around each centroid. Furthermore, the proposed Terrain Surface Interpolation method searches for heavy construction equipment points (Class 3) located within the ground region (Class 1) and creates the same number of clusters as the number of detected construction equipment instances. In this process, the radius (r) can be specified using an arbitrary user-defined value. This process enables the simultaneous detection and interpolation of multiple heavy construction equipment units in the dataset. To determine the adjusted Z-values for the Class 3 points within each cluster, the average Z-value of the surrounding ground points (Class 1) within the cluster r is calculated and applied to the heavy construction equipment points.

In this way, the proposed terrain surface interpolation method performs height adjustment without deleting the heavy construction equipment points, thereby preserving data continuity. Additionally, in the same manner as the Z-value adjustment, the color information (R, G, B) and point density of the predicted data within each cluster are averaged and applied to the interpolated region. Through this approach, the interpolated heavy construction equipment points obtain color and density values similar to their surrounding

terrain, ensuring uniform point distribution across the dataset. In particular, conventional methods that remove heavy construction equipment point clouds and generate flat terrain surfaces often create holes in the dataset. When using point generation methods to fill these holes, it is difficult to maintain uniform density, which can result in data loss and high computational costs. In contrast, the proposed terrain surface interpolation method effectively fills these holes with uniform density while significantly reducing processing time compared with conventional methods.

3.4. Selection of Earthwork Volume Estimation Method

After performing terrain surface interpolation, this research proceeded to estimate the earthwork volume from the 3D point cloud data. The procedure for earthwork volume estimation was conducted in the following order: (1) preparation of interpolated 3D point cloud data, (2) calculation of the earthwork volume, and (3) verification of the calculated results. For a detailed explanation of this process, the 3D point cloud data subjected to terrain surface interpolation was first prepared. When estimating earthwork quantities from multiple 3D point cloud datasets, a preprocessing step was carried out to ensure that the horizontal and vertical extents of all datasets were identical so that each dataset covered the same surface area. Finally, the prepared 3D point cloud data was processed using specialized software for earthwork volume estimation.

In particular, to ensure accurate earthwork volume estimation using large-scale 3D point cloud data, this study reviewed previous research [28]. The review indicated that among various software platforms, CloudCompare demonstrated the most superior performance, as it employs the 2.5D Volume algorithm. Accordingly, CloudCompare v2.12 alpha [28] was adopted in this research, and a raster size of 0.005 m was applied under identical conditions to minimize potential volume estimation differences or computational errors during analysis.

4. Experimental Result and Discussion

4.1. Experimental Setup

In this chapter, an experiment was conducted to verify the performance of the developed terrain surface interpolation method. As shown in Figure 3, the experiment was carried out in the following sequence: construction of time-series 3D point cloud data, development of the semantic segmentation model, execution of terrain surface interpolation, change detection analysis, and finally, earthwork volume estimation. In particular, to clearly evaluate the performance of the proposed interpolation method, change detection analysis was included in addition to earthwork volume estimation. Accordingly, this chapter provides a detailed description of each experimental step, from Sections 4.2–4.4. In Section 4.4, a comprehensive analysis is presented, including the outcomes of the terrain surface interpolation, the change detection analysis using time-series data, and the earthwork volume estimation based on the interpolated datasets.

4.2. Generation of Predicted Data

In this experiment, photogrammetry was conducted using a UAV to construct the dataset required for analysis. The selected construction site, as shown in Figure 4, is a road construction site located near Gwangju, Gyeonggi-do, Republic of Korea, which was in the earthwork phase at the time of data acquisition. The UAV used in this study was a PHANTOM 4 manufactured by DJI, equipped with Real-Time Kinematic Global Navigation Satellite System (RTK GNSS) to ensure precise data collection. To obtain reliable and accurate data, multiple photogrammetric surveys were performed at the same construction site at intervals of approximately one week. During each flight, the drone operated at an altitude

of approximately 100 m, and the integration of RTK GNSS allowed the acquisition of highly accurate and high-quality topographic data for subsequent 3D point cloud generation.

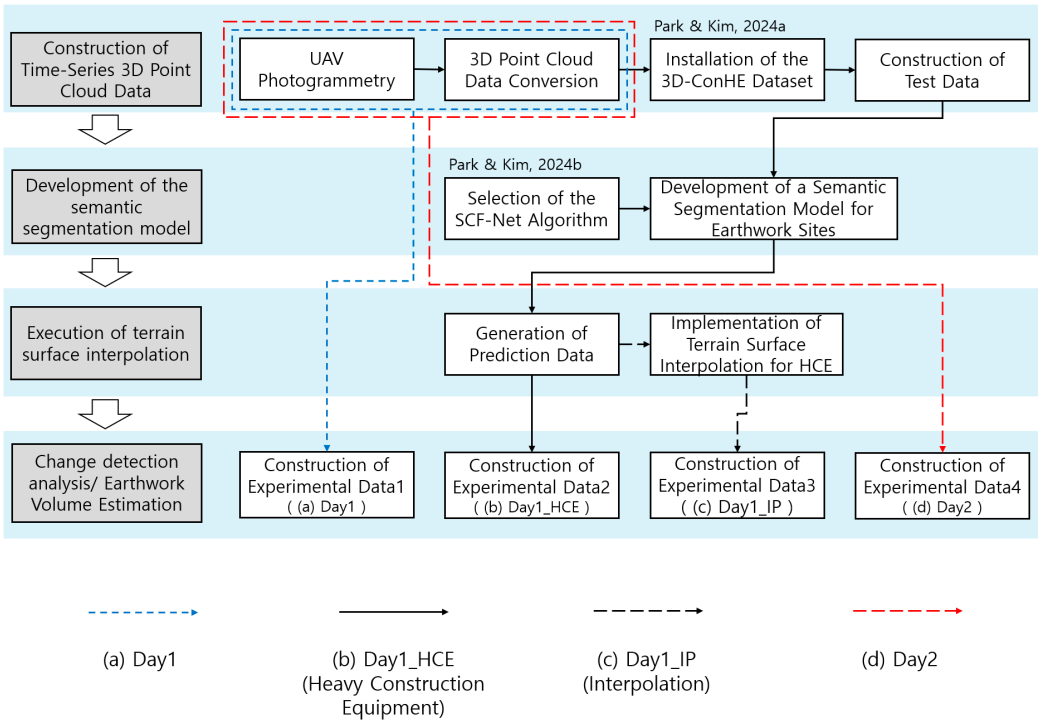


Figure 3. Process of the Experiment [22,23].

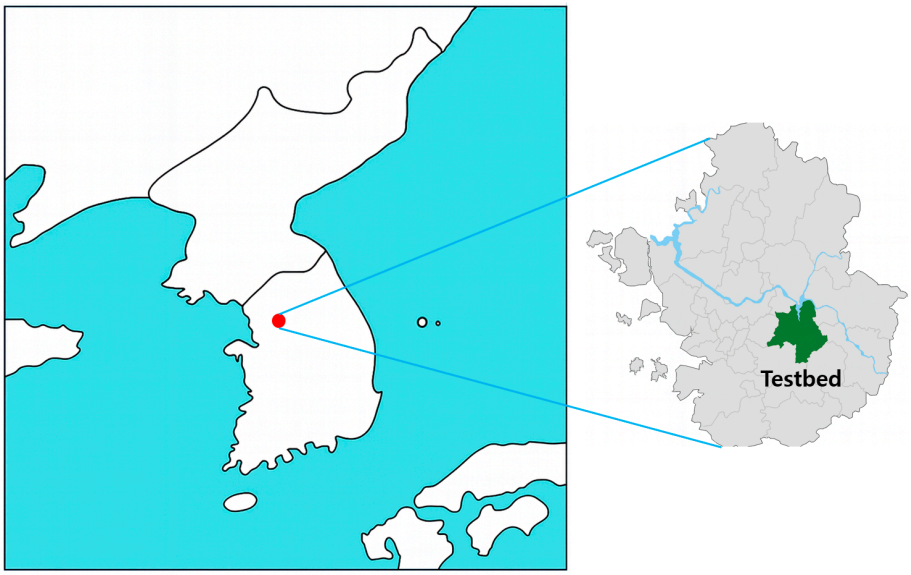


Figure 4. Location of the Experiment Testbed.

In this Experiment, the photogrammetric data acquired from the road construction site were post-processed to convert them into 3D point cloud data and to remove noise. For this task, Pix4Dmapper v4.10 [38] was utilized, and the output data were stored in the *.LAS file format. Among the acquired 3D point cloud datasets, two were selected that contained minimal construction workers and heavy construction equipment, in order to minimize errors in earthwork volume estimation caused by large obstacles. Additionally, datasets captured at different times were selected to clearly observe changes in earthwork volumes, such as embankment and excavation, within the testbed. As the final step in constructing

the experimental dataset, six heavy construction equipment objects from the 3D-ConHE Dataset [22], developed in the authors' previous research, were virtually placed on the ground surface of Day 1 data. Through this process, experimental data were designed to replicate actual working conditions, with heavy construction equipment operating on an active earthwork site.

The experimental data constructed for this research consisted of large-scale 3D point cloud data in *.LAS file format. Two datasets (Day 1 and Day 2) were created from the same construction site, with Day 1 being captured seven days prior to Day 2. Each dataset covered an area of approximately 340 m (width) × 510 m (length) × 90 m (height), with a total file size of 853 MB and containing 40,755,652 points. To prepare the data for semantic segmentation prediction, the *.LAS files were converted to *.TXT format for input into the trained model.

As described in Section 3, this Experiment adopted the semantic segmentation model trained in the authors' previous research [23] to improve computational efficiency and maintain methodological consistency. The SCF-Net algorithm [34] was employed as the backbone network, which demonstrated superior performance in identifying heavy construction equipment in large-scale 3D point cloud datasets [23]. The trained SCF-Net–based model was tested using the Day 1 data to generate predicted data for this research. The testing environment consisted of Ubuntu 16.04 LTS, Python 3.6.13, TensorFlow 1.11.0, and one NVIDIA GeForce GTX 1080 Ti (11 GB) GPU. The hyperparameters for testing were set identical to those used in the previous study [23]. As a result, predicted data (Day 1) were successfully generated and prepared for the subsequent Terrain Surface Interpolation process.

4.3. Results of Terrain Surface Interpolation

Subsequently, the terrain surface interpolation method developed in this research was applied to the predicted data generated from the 3D semantic segmentation model. As described in Section 3.3, the interpolation in this experiment was performed using predicted data generated from a large-scale 3D point cloud–based semantic segmentation model. In particular, the interpolation process targeted the 3D point cloud data of heavy construction equipment, adjusting their Z-values to match the elevation of the surrounding ground surface, thereby completing the experimental dataset. The results before and after applying the developed interpolation method can be visually confirmed in Figures 5 and 6.



Figure 5. Before Terrain Surface Interpolation.



Figure 6. After Terrain Surface Interpolation.

As shown in Figure 5, all six heavy construction equipment objects were successfully interpolated, achieving Z-values and point densities consistent with the surrounding terrain. Furthermore, despite the uneven and sloped ground surface of the earthwork site, as depicted in Figures 5 and 6, the interpolation was effectively performed, demonstrating stable terrain reconstruction performance. However, in some cases where construction equipment was located on sloped surfaces, slight discrepancies were observed between the interpolated terrain and the actual ground slope. Nevertheless, the terrain interpolation technique developed in this research demonstrated consistent correction of Z-values even when applied simultaneously to multiple pieces of heavy construction equipment. In addition, the color information (R, G, B) and point densities of the interpolated points were also found to be similar to those of the surrounding terrain. The interpolation process required less than 3 min to complete a single file under 500 MB, demonstrating high computational efficiency. However, as illustrated in Figure 6, several points located on the wheels and lower parts of the heavy construction equipment were not fully interpolated. This issue is considered to have occurred because some of these points were not recognized as heavy construction equipment during the prediction phase of the 3D semantic segmentation model. This finding suggests a strong interdependence between the object recognition performance of the semantic segmentation model and the accuracy of the proposed terrain surface interpolation method.

4.4. Results of Terrain Change Analysis

After performing terrain interpolation, the terrain change analysis was conducted using the 3D point cloud data of the earthwork site that had undergone terrain interpolation. The experimental datasets used for this analysis are shown in Figure 7a–d, and their detailed descriptions are as follows. First, Figure 7a represents the 3D point cloud data of the construction site without heavy construction equipment, serving as the baseline dataset. Figure 7b shows the dataset predicted by the 3D semantic segmentation model developed in this research, which includes heavy construction equipment and serves as the target data for terrain interpolation. Figure 7c presents the terrain-interpolated result of Figure 7b, where the proposed terrain surface interpolation method was applied to adjust the Z-values of heavy construction equipment to match the surrounding ground surface. These three datasets were generated from the same earthwork site 3D point cloud data, differing only in (1) the presence or absence of heavy construction equipment, (2) whether the semantic segmentation method was applied, and (3) whether terrain interpolation was conducted. Finally, Figure 7d represents the 3D point cloud data captured seven days after Figure 7a, reflecting the actual progress of earthwork activities at the site. Initially,

the entire area displayed in Figure 7a–d was considered for the terrain change analysis. However, as shown in the figures, the datasets included several non-construction regions such as forested areas, farmland, and road sections that were irrelevant to the earthwork process. Accordingly, as shown in Figure 7a–d, the region outlined with red dotted lines, where earthwork activities were concentrated, was designated as the target area for the terrain change analysis.

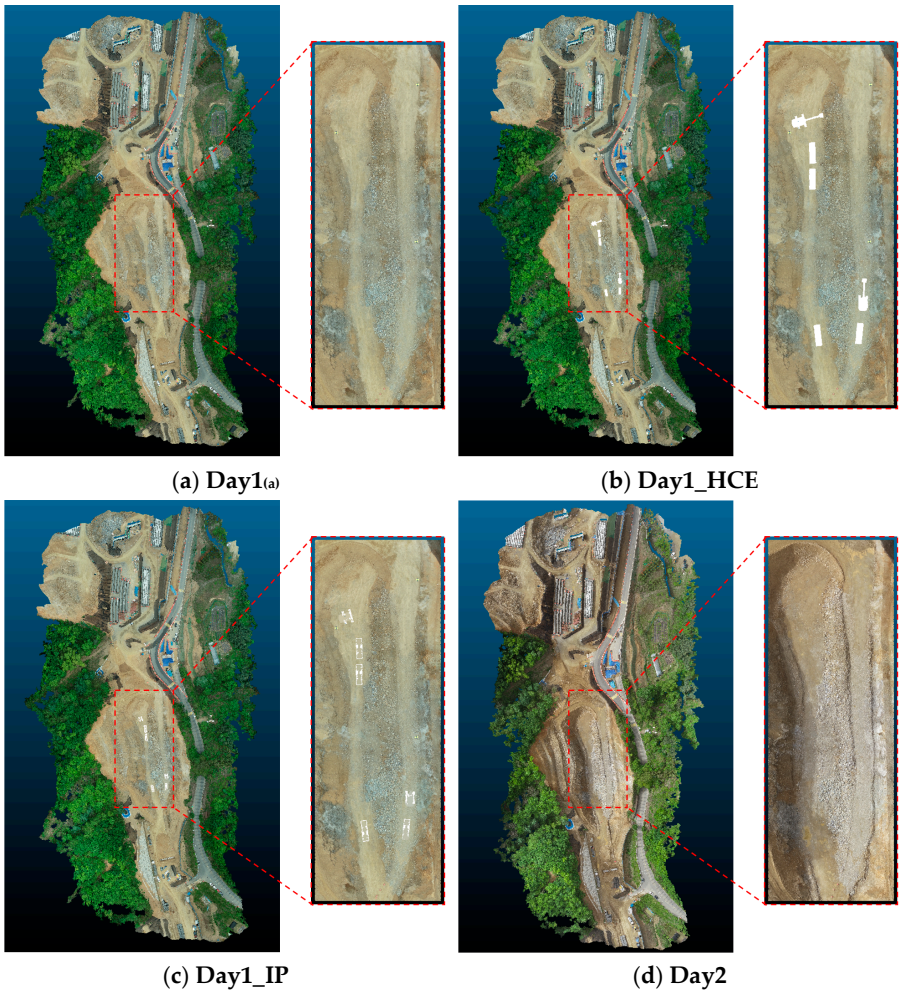


Figure 7. Selection of the Target Area for Terrain Change Analysis.

For the terrain change analysis(Figure 8a–f), the C2C (Cloud-to-Cloud) algorithm was employed [19]. This method was selected because the C2C-based terrain change analysis approach is widely utilized and well-suited for analyzing large-scale 3D point cloud data of earthwork sites [7,39,40]. The analysis was conducted using CloudCompare software [32], with the maximum distance (Z-value range) parameter set to 1.45 m. This threshold was determined based on the height range observed in the experimental datasets (Figure 7a–d) to achieve optimal visual representation of terrain differences. In Figure 8a–d, the blue regions indicate relatively small height differences, whereas the red regions represent height variations of approximately 1.4 m. The analysis procedure was as follows: Figure 7d, representing the latest dataset, was used as the reference, and the other datasets (Figure 7a–c) were sequentially compared against it. Specifically, Figure 7a was compared with Figure 7d to analyze terrain changes without heavy construction equipment, Figure 7b was compared with Figure 7d to examine terrain changes with Heavy Construction Equipment, and Figure 7c was compared with Figure 7d to evaluate terrain changes after terrain surface interpolation of heavy construction equipment regions. The results of these three

comparative analyses were visualized and summarized in Figure 7, using both spatial color maps and histogram representations. Figure 7a shows the visual analysis result obtained from comparing Figure 7a,d, while Figure 7b presents the corresponding histogram of the same comparison. Following the same approach, the remaining terrain change analysis results were organized accordingly.

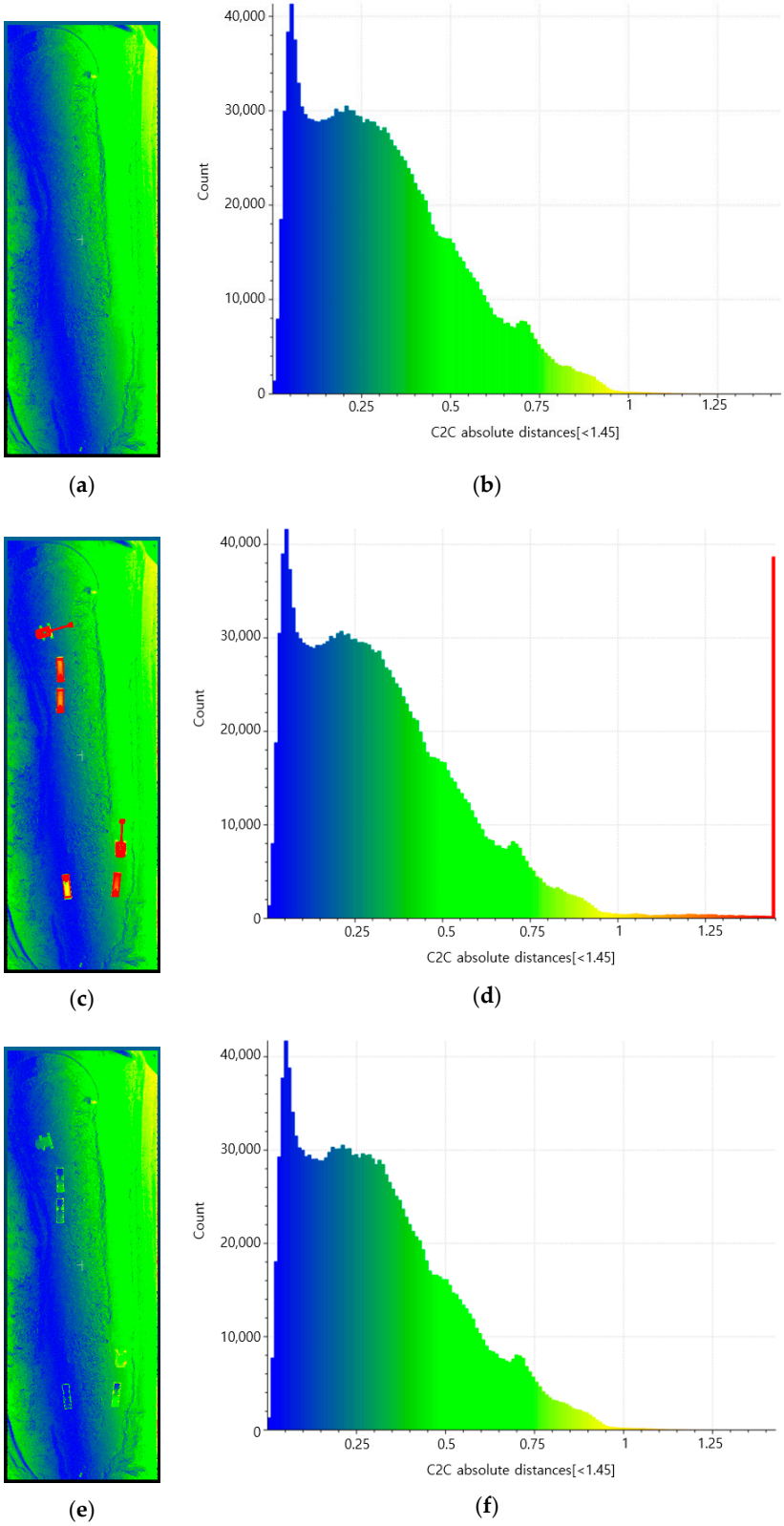


Figure 8. Results of Terrain Change Analysis.

As illustrated in Figure 8c, when compared with Figure 8a, the heavy construction equipment is highlighted in red, indicating areas where the 3D point cloud data of heavy construction equipment were erroneously interpreted as embankment zones during the terrain change analysis. This misclassification is more evident in Figure 8d, where the histogram shows a sharp increase in red-colored points beyond 1 m on the *X*-axis (representing the absolute distance between points), whereas the *Y*-axis indicates the number of accumulated points. Unlike Figure 8b, where the distribution below 1 m remains consistent, the histogram in Figure 8d displays a noticeable spike beyond 1 m, attributed to the presence of heavy construction equipment points. In contrast, the results shown in Figure 8e,f —which correspond to the terrain-interpolated datasets—demonstrate that most of these red-colored artifacts have been removed, leaving only minimal traces of heavy construction equipment. These findings confirm that the proposed terrain surface interpolation method effectively restores ground elevation and maintains high-quality terrain correction, even when applied simultaneously to multiple heavy construction equipment objects within large-scale 3D point cloud datasets.

4.5. Earthwork Volume Estimation Results

Subsequently, terrain surface interpolation and terrain change analysis were performed, followed by the earthwork volume estimation using 3D point cloud data. The same experimental datasets (Figure 7a–d) used in the terrain interpolation experiment were employed in this earthwork volume estimation. This experiment was conducted not only to visually verify the results of the terrain-interpolation process but also to quantitatively evaluate the performance of the proposed interpolation method through numerically derived earthwork volumes. The datasets used for this experiment correspond to the red-dotted rectangular area shown within Figure 7a–d. All four datasets share the same 7100 m^2 area (50 m $\times$ 142 m). The estimation was carried out using CloudCompare v2.12 alpha software [32].

The results of the earthwork volume estimation are summarized in Table 1. All sections consisted solely of cut (excavation) areas, with no fill (embankment) detected. The estimated earthwork volumes were as follows: Day 1—109,953 m^3, Day 1_HCE (Heavy Construction Equipment) 109,718 m^3, Day 1_IP (Interpolation)—109,940 m^3, and Day 2—111,713 m^3. When comparing these four cases, the volume difference between Day 1 and Day 2 was 1760 m^3; between Day 1_HCE and Day 2 was 1995 m^3; and between Day 1_IP and Day 2 was 1773 m^3. Comparing these differences, the discrepancy between (A) and (B) was 235 m^3, whereas the discrepancy between (A) and (C) was only 13 m^3.

Table 1. Results of Earthwork Volume Estimation.

Data	Number of Points	Volume (m^3)	Volume Difference to Day2 (m^3)
Day1	1,654,440	109,953	(A) 1760
Day1_HCE	1,715,015	109,718	(B) 1995
Day1_IP	1,715,015	109,940	(C) 1773
Day2	1,756,926	111,713	-

This indicates that the difference was reduced by approximately 94% when applying the proposed terrain-interpolation method, demonstrating a significant reduction in earthwork volume estimation error. Additionally, as shown in Table 1, Day 1_HCE and Day 1_IP have the same number of points. Therefore, based on these experimental results, it can be concluded that the proposed terrain-interpolation method enables accurate and reliable earthwork volume estimation from large-scale 3D point cloud datasets without point-loss.

5. Conclusions

This research proposed and validated a semantic segmentation-based terrain surface interpolation and earthwork volume estimation method using large-scale 3D point cloud data. Unlike labor-intensive terrain interpolation methods that are manually performed to delete and regenerate unnecessary objects such as heavy construction equipment, the proposed approach performs terrain interpolation by utilizing 3D semantic segmentation prediction data, while simultaneously adjusting the height, color, and point density of the objects during the interpolation process. Through this new approach, the proposed method minimizes data loss and enables efficient and precise terrain interpolation for large-scale 3D point cloud datasets. In particular, this research systematically performed 3D semantic segmentation, terrain interpolation, terrain change detection, and earthwork volume estimation using UAV photogrammetry-based 3D point cloud data acquired from an actual earthwork construction site.

As a result of these field experiments, the proposed terrain interpolation method effectively harmonized the point clouds of heavy construction equipment with the surrounding terrain, producing visually natural and coherent interpolation outcomes. In addition, the earthwork volume estimation experiment demonstrated that the 3D point cloud data with the proposed interpolation method reduced earthwork estimation errors by approximately 94% compared to data without interpolation. These results confirm that the proposed interpolation approach can significantly reduce potential errors in 3D point cloud-based earthwork volume estimation, thereby enabling efficient, accurate, and reliable estimation outcomes. However, this research has a limitation in that the 3D-ConHE dataset rather than actual point cloud data of heavy construction equipment was used for the terrain interpolation experiments. Therefore, future research will focus on conducting additional field experiments using actual 3D point cloud data containing heavy construction equipment to verify the on-site applicability and robustness of the proposed method. Furthermore, additional research is required to evaluate the accuracy of earthwork volume estimation when applying the proposed terrain interpolation method. It is expected that the outcomes of this research will serve as a foundation for future studies on construction automation utilizing large-scale 3D point cloud data.

Author Contributions: Literature review, S.P.; writing—original draft preparation, S.P.; proposal of the overall framework and direction of the research, S.K.; writing—review and editing, S.K.; dataset generation S.P.; data analysis, Y.K.; data analysis review, S.P. and S.K. All authors have read and agreed to the published version of the manuscript.

Funding: This research received no external funding.

Data Availability Statement: The original contributions presented in this study are included in the article. Further inquiries can be directed to the corresponding author.

Acknowledgments: This research was conducted with the support of the "National R&D Project for Smart Construction Technology (No. RS-2020-KA156875)" funded by the Korea Agency for Infrastructure Technology Advancement under the Ministry of Land, Infrastructure and Transport, and managed by the Korea Expressway Corporation.

Conflicts of Interest: The authors declare no conflicts of interest.

References

1. Du, J.C.; Teng, H.C. 3D Laser Scanning and GPS Technology for Landslide Earthwork Volume Estimation. *Autom. Constr.* **2007**, *16*, 657–663. [CrossRef]
2. Lichti, D.D.; Gordon, S.J.; Stewart, M.P. Ground-Based Laser Scanners: Operation, System and Applications. *Geomatica* **2002**, *56*, 21–33.

3. Prakash, A.; Verma, A.; Sharma, A.; Jaiswal, P.; Mandal, S.K. A Hybrid of GNSS Remote Sensing and Ground-Based Laser Technology for Geo-Referenced Surveying in Mining. *Curr. Sci.* **2024**, *126*, 336–344. [CrossRef]
4. Ersoz, A.B.; Pekcan, O. UAV-Based Automated Earthwork Progress Monitoring Using Deep Learning with Image Inpainting. *Autom. Constr.* **2025**, *175*, 106211. [CrossRef]
5. Hasegawa, H.; Sujaswara, A.A.; Kanemoto, T.; Tsubota, K. Possibilities of Using UAV for Estimating Earthwork Volumes during Process of Repairing a Small-Scale Forest Road, Case Study from Kyoto Prefecture, Japan. *Forests* **2023**, *14*, 677. [CrossRef]
6. Chonpatathip, S.; Suanpaga, W.; Muttitanon, W. Earthwork Volume Measurement in Road Construction Using Unmanned Aerial Vehicle (UAV). *Int. J. Geoinform.* **2023**, *19*, 51–64. [CrossRef]
7. Winiwarter, L.; Anders, K.; Wujanz, D.; Höfle, B. Influence of Ranging Uncertainty of Terrestrial Laser Scanning on Change Detection in Topographic 3D Point Clouds. *ISPRS Ann. Photogramm. Remote Sens. Spat. Inf. Sci.* **2020**, *5*, 789–796. [CrossRef]
8. Kastens, K.; Kaplan, D.; Christien-Blick, K. Development and Evaluation of High-Precision Earth-Work Calculating System Using Drone Survey. *J. Geosci. Educ.* **2001**, *49*, 249–266. [CrossRef]
9. Lee, S.B.; Han, D.; Song, M. Calculation and Comparison of Earthwork Volume Using Unmanned Aerial Vehicle Photogrammetry and Traditional Surveying Method. *Sensors Mater.* **2022**, *34*, 4737–4753. [CrossRef]
10. Kim, Y.; Park, S.; Choi, Y.; Kim, S. Performance Verification of Integrated Module for Automatic Analysis of Digital Maps in Earthwork Sites. *J. Constr. Autom. Robot.* **2023**, *2*, 1–6. [CrossRef]
11. Kim, G.; Choi, S.; Kim, A. Scan Context++: Structural Place Recognition Robust to Rotation and Lateral Variations in Urban Environments. *IEEE Trans. Robot.* **2022**, *38*, 1856–1874. [CrossRef]
12. Dai, A.; Ritchie, D.; Bokeloh, M.; Reed, S.; Sturm, J.; Niebner, M. ScanComplete: Large-Scale Scene Completion and Semantic Segmentation for 3D Scans. In Proceedings of the IEEE Conference on Computer Vision and Pattern Recognition, Salt Lake City, UT, USA, 18–22 June 2018; pp. 4578–4587. [CrossRef]
13. Mirzaei, K.; Arashpour, M.; Asadi, E.; Masoumi, H.; Bai, Y.; Behnood, A. 3D Point Cloud Data Processing with Machine Learning for Construction and Infrastructure Applications: A Comprehensive Review. *Adv. Eng. Inform.* **2022**, *51*, 101501. [CrossRef]
14. Kim, Y.-G.; Park, S.-Y.; Kim, S. Development of Framework for Digital Map Time Series Analysis of Earthwork Sites. *J. KIBIM* **2023**, *13*, 22–32. [CrossRef]
15. Choi, Y.; Park, S.; Kim, S. GCP-Based Automated Fine Alignment Method for Improving the Accuracy of Coordinate Information on UAV Point Cloud Data. *Sensors* **2022**, *22*, 8735. [CrossRef] [PubMed]
16. Bello, S.A.; Yu, S.; Wang, C.; Adam, J.M.; Li, J. Review: Deep Learning on 3D Point Clouds. *Remote Sens.* **2020**, *12*, 1729. [CrossRef]
17. Guo, Y.; Wang, H.; Hu, Q.; Liu, H.; Liu, L.; Bennamoun, M. Deep Learning for 3D Point Clouds: A Survey. *IEEE Trans. Pattern Anal. Mach. Intell.* **2021**, *43*, 4338–4364. [CrossRef]
18. Lee, J.S.; Park, J.; Ryu, Y.M. Semantic Segmentation of Bridge Components Based on Hierarchical Point Cloud Model. *Autom. Constr.* **2021**, *130*, 103847. [CrossRef]
19. Kharroubi, A.; Poux, F.; Ballouch, Z.; Hajji, R.; Billen, R. Three Dimensional Change Detection Using Point Clouds: A Review. *Geomatics* **2022**, *2*, 457–485. [CrossRef]
20. Lague, D.; Brodu, N.; Leroux, J. Accurate 3D Comparison of Complex Topography with Terrestrial Laser Scanner: Application to the Rangitikei Canyon (N-Z). *ISPRS J. Photogramm. Remote Sens.* **2013**, *82*, 10–26. [CrossRef]
21. Kim, H.; Kim, C. Deep-Learning-Based Classification of Point Clouds for Bridge Inspection. *Remote Sens.* **2020**, *12*, 3757. [CrossRef]
22. Park, S.; Kim, S. 3D Point Cloud Dataset of Heavy Construction Equipment. *Appl. Sci.* **2024**, *14*, 3599. [CrossRef]
23. Park, S.; Kim, S. Semantic Segmentation of Heavy Construction Equipment Based on Point Cloud Data. *Buildings* **2024**, *14*, 2393. [CrossRef]
24. Hu, Q.; Yang, B.; Xie, L.; Rosa, S.; Guo, Y.; Wang, Z.; Trigoni, N.; Markham, A. Randla-Net: Efficient Semantic Segmentation of Large-Scale Point Clouds. In Proceedings of the IEEE/CVF Conference on Computer Vision and Pattern Recognition, Seattle, WA, USA, 14–19 June 2020; pp. 11105–11114. [CrossRef]
25. Hackel, T.; Savinov, N.; Ladicky, L.; Wegner, J.D.; Schindler, K.; Pollefeys, M. Semantic3d.net: A new large-scale point cloud classification. *arXiv* **2014**, arXiv:1704.03847. [CrossRef]
26. Nguyen, V.S.; Tran, M.H.; Nguyen, T.T. Filling Holes on the Surface of 3D Point Clouds Based on Tangent Plane of Hole Boundary Points. In Proceedings of the 7th Symposium on Information and Communication Technology, Ho Chi Minh, Vietnam, 8–9 December 2016; pp. 331–338. [CrossRef]
27. Emmitt, J.; Pillay, P.; Barrett, M.; Middleton, S.; Mackrell, T.; Floyd, B.; Ladefoged, T.N. A Comparison of Volumetric Reconstruction Methods of Archaeological Deposits Using Point-Cloud Data from Ahuahu, Aotearoa New Zealand. *Remote Sens.* **2021**, *13*, 4015. [CrossRef]
28. Štroner, M.; Křemen, T.; Braun, J.; Urban, R.; Blistan, P.; Kovanič, L. Comparison of 2.5d Volume Calculation Methods and Software Solutions Using Point Clouds Scanned before and after Mining. *Acta Montan. Slovaca* **2019**, *24*, 296–306.
29. Idrees, A.; Heeto, F. Evaluation of Uav-Based Dem for Volume Calculation. *J. Univ. Duhok* **2020**, *23*, 11–24. [CrossRef]

30. Leica Geosystems. Leica Cyclone 3DR. Available online: https://leica-geosystems.com/en-us/products/laser-scanners/software/leica-cyclone/leica-cyclone-3dr?utm_source=chatgpt.com (accessed on 4 October 2025).
31. Trimble Inc. Trimble RealWorks. Available online: https://geospatial.trimble.com/en/products/software/trimble-realworks?utm_source=chatgpt.com (accessed on 4 October 2025).
32. Girardeau-montaut, D. *CloudCompare*; EDF R&D Telecom ParisTech: Paris, France, 2019.
33. Skabek, K.; Kowalski, P. Building the Models of Cultural Heritage Objects Using Multiple 3D Scanners. *Theor. Appl. Inform.* **2009**, *21*, 115–129.
34. Fan, S.; Dong, Q.; Zhu, F.; Lv, Y.; Ye, P.; Wang, F.Y. SCF-Net: Learning Spatial Contextual Features for Large-Scale Point Cloud Segmentation. In Proceedings of the IEEE/CVF Conference on Computer Vision and pattern Recognition, Nashville, TN, USA, 19–25 June 2021; pp. 14499–14508. [CrossRef]
35. Kolodiazhnyi, M.; Vorontsova, A.; Konushin, A.; Rukhovich, D. OneFormer3D: One Transformer for Unified Point Cloud Segmentation. In Proceedings of the IEEE/CVF Conference on Computer Vision and Pattern Recognition, Vancouver, BC, Canada, 18–22 June 2023; pp. 20943–20953.
36. Zhang, H.; Wang, C.; Yu, L.; Tian, S.; Ning, X.; Member, S.; Rodrigues, J. PointGT: A Method for Point-Cloud Classification and Segmentation Based on Local Geometric Transformation. *IEEE Trans. Multimed.* **2024**, *26*, 8052–8062. [CrossRef]
37. Zhao, L.; Hu, Y.; Yang, X.; Dou, Z.; Kang, L. Robust Multi-Task Learning Network for Complex LiDAR Point Cloud Data Preprocessing. *Expert Syst. Appl.* **2024**, *237*, 121552. [CrossRef]
38. Pix4D SA Pix4Dmapper. Available online: https://www.pix4d.com/product/pix4dmapper-photogrammetry-software/?utm_source=chatgpt.com (accessed on 4 October 2025).
39. Qin, R.; Tian, J.; Reinartz, P. 3D Change Detection—Approaches and Applications. *ISPRS J. Photogramm. Remote Sens.* **2016**, *122*, 41–56. [CrossRef]
40. Fuse, T.; Yamano, T. Change Detection of Time-Series 3D Point Clouds Using Robust Principal Component Analysis. *Int. Arch. Photogramm. Remote Sens. Spat. Inf. Sci.—ISPRS Arch.* **2021**, *43*, 163–169. [CrossRef]

Disclaimer/Publisher's Note: The statements, opinions and data contained in all publications are solely those of the individual author(s) and contributor(s) and not of MDPI and/or the editor(s). MDPI and/or the editor(s) disclaim responsibility for any injury to people or property resulting from any ideas, methods, instructions or products referred to in the content.